# 高精度粲偶素谱学研究新进展

刘 翔
xiangliu@lzu.edu.cn
兰州大学

“第十届XYZ研讨会”
长沙 2024年4月11日-15日

# Outline

- Background
- Mixing scheme for $\psi(4220)$ induced by a coupled-channel approach
- Reevaluating the $\psi(4160)$ resonance parameter
- Discovery potential of charmonium 2P states through $e^+e^- \to \omega D\bar{D}$ and $e^+e^- \to \gamma D\bar{D}$
- Non-$D\bar{D}$ decays of $\psi_3(3842)$
- Summary

# 1. Background

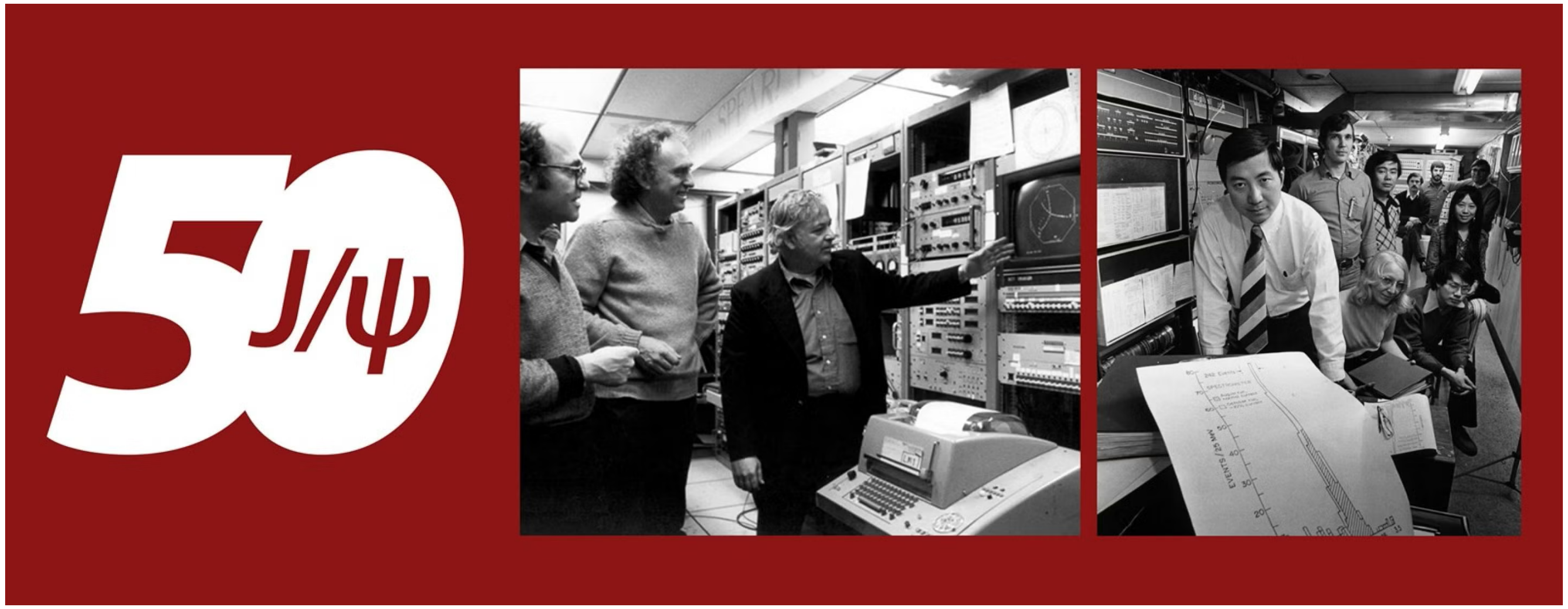


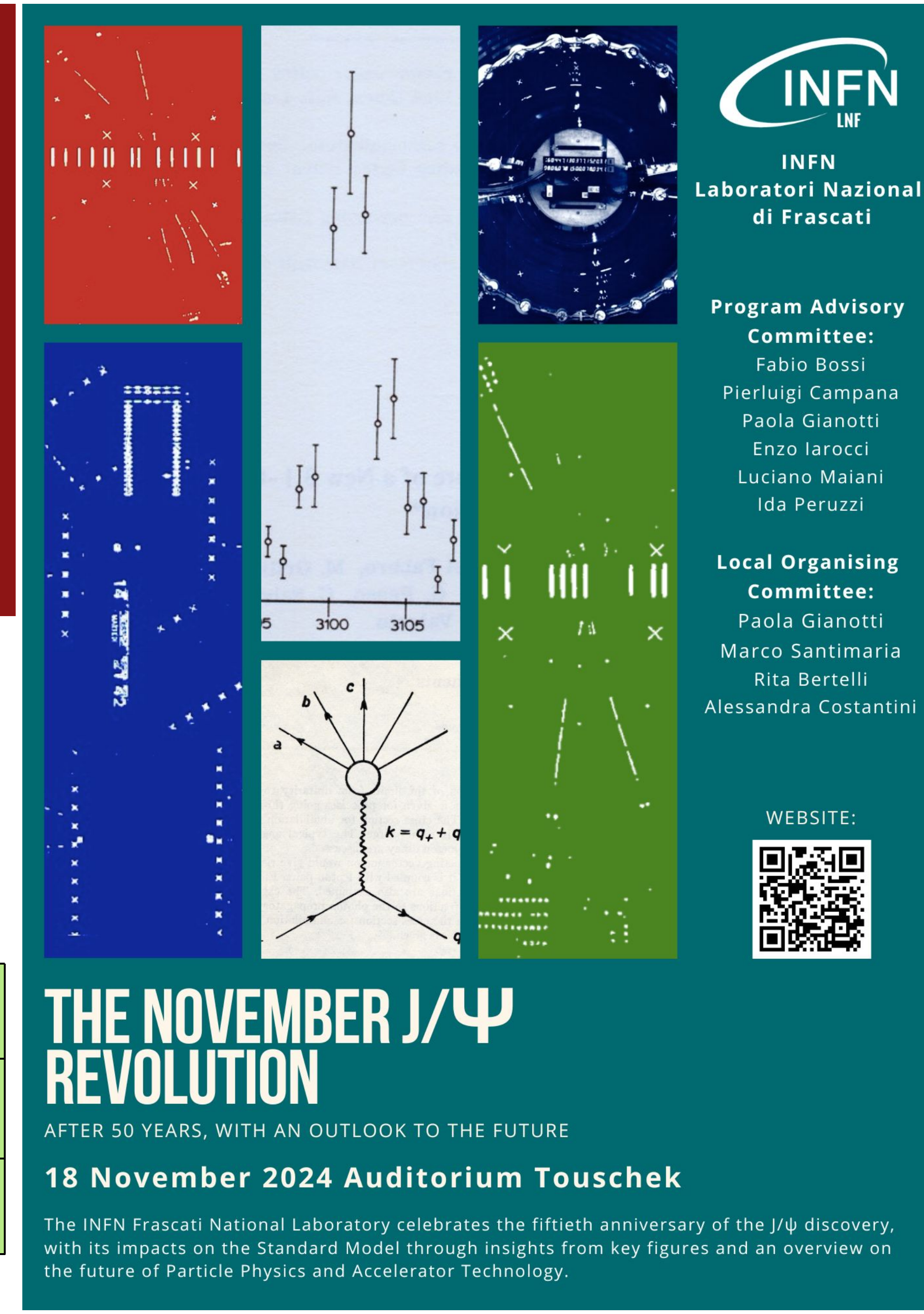


| | | | | | | | | | | | | | | | | | |
|---|---|---|---|---|---|---|---|---|---|---|---|---|---|---|---|---|---|
| $6^1S_0$ | $6^3S_1$ | $6^1P_1$ | $6^3P_0$ $\chi_{c0}(4700)$ $4694^{+16}_{-5}$ $87^{+18}_{-10}$ | $6^3P_1$ $\chi_{c1}(4685)$ $4684 \pm 15$ $130 \pm 40$ | $6^3P_2$ | $6^3D_1$ | | | | | | | | | | | |
| $5^1S_0$ | $5^3S_1$ $\psi(4415)$ $4415 \pm 5$ $110 \pm 22$ | $5^1P_1$ | $5^3P_0$ $\chi_{c0}(4500)$ $4474 \pm 4$ $77 \pm 10$ | $5^3P_1$ | $5^3P_2$ | $5^3D_1$ $\psi(4660)$ $4641 \pm 10$ $73 \pm 11$ | | | | | | | | | | | |
| $4^1S_0$ | $4^3S_1$ $\psi(4230)$ $4222 \pm 2.3$ $49 \pm 7$ | $4^1P_1$ | $4^3P_0$ | $4^3P_1$ $\chi_{c1}(4274)$ $4286 \pm 8.0$ $51 \pm 7$ | $4^3P_2$ | $4^3D_1$ $\psi(4500)$ $4469 \pm 26$ $246 \pm 36$ | | | | | | | | | | | |
| $3^1S_0$ | $3^3S_1$ $\psi(4040)$ $4040 \pm 4$ $84 \pm 12$ | $3^1P_1$ | $3^3P_0$ | $3^3P_1$ $\chi_{c1}(4140)$ $4146 \pm 3.0$ $19^{+7}_{-5}$ | $3^3P_2$ | $3^3D_1$ $\psi(4360)$ $4374 \pm 7$ $118 \pm 12$ | $3^3D_2$ | $3^3D_3$ | $3^1D_2$ | $3^1F_3$ | $3^3F_2$ | $3^3F_3$ | $3^3F_4$ | $3^1G_4$ | $3^3G_3$ | $3^3G_4$ | $3^3G_5$ |
| $2^1S_0$ $\eta_c(2S)$ $3637 \pm 0.9$ $11.8 \pm 1.6$ | $2^3S_1$ $\psi(2S)$ $3686 \pm 0.011$ $0.293 \pm 0.009$ | $2^1P_1$ | $2^3P_0$ $\chi_{c0}(3915)$ $3922 \pm 0.18$ $20 \pm 4$ | $2^3P_1$ $\chi_{c1}(3872)$ $3871 \pm 0.06$ $1.19 \pm 0.21$ | $2^3P_2$ $\chi_{c2}(3930)$ $3922 \pm 1.0$ $35.2 \pm 2.2$ | $2^3D_1$ $\psi(4160)$ $4191 \pm 5$ $69 \pm 10$ | $2^3D_2$ | $2^3D_3$ | $2^1D_2$ | $2^1F_3$ | $2^3F_2$ | $2^3F_3$ | $2^3F_4$ | $2^1G_4$ | $2^3G_3$ | $2^3G_4$ | $2^3G_5$ |
| $1^1S_0$ $\eta_c$ $2984 \pm 0.4$ $30.5 \pm 0.5$ | $1^3S_1$ $J/\psi$ $3096 \pm 0.006$ $0.093 \pm 0.002$ | $1^1P_1$ $h_c(1P)$ $3525 \pm 0.14$ $0.78 \pm 0.28$ | $1^3P_0$ $\chi_{c0}(1P)$ $3414 \pm 0.3$ $10.7 \pm 0.6$ | $1^3P_1$ $\chi_{c1}(1P)$ $3510 \pm 0.05$ $0.84 \pm 0.04$ | $1^3P_2$ $\chi_{c2}(1P)$ $3556 \pm 0.07$ $1.98 \pm 0.09$ | $1^3D_1$ $\psi(3770)$ $3773 \pm 0.7$ $27.2 \pm 1.0$ | $1^3D_2$ $\psi_2(3823)$ $3823 \pm 0.34$ $< 2.9$ | $1^3D_3$ $\psi_3(3842)$ $3842 \pm 0.2$ $2.8 \pm 0.6$ | $1^1D_2$ | $1^1F_3$ | $1^3F_2$ | $1^3F_3$ | $1^3F_4$ | $1^1G_4$ | $1^3G_3$ | $1^3G_4$ | $1^3G_5$ |
| $0^{-+}$ | $1^{--}$ | $1^{+-}$ | $0^{++}$ | $1^{++}$ | $2^{++}$ | $1^{--}$ | $2^{--}$ | $3^{--}$ | $2^{-+}$ | $3^{+-}$ | $2^{++}$ | $3^{++}$ | $4^{++}$ | $4^{-+}$ | $3^{--}$ | $4^{--}$ | $5^{--}$ |

Quantum number
($n^{2S+1}L_J$)
State
Mass (MeV)
Width (MeV)

- Candidate states
- Established states
- Our focused states
- Missing states

1974 — $J/\psi$

1978 — Cornel potential

2003 — XYZ states

**Challenges and opportunities**

# 2. Mixing scheme for $\psi(4220)$ induced by a coupled-channel approach

A slide from my presentation at the XYZ workshop in Xi'an

**2. Now** | **Unquenched potential model**

## Introducing 4S-3D mixing scheme

$$\begin{pmatrix} |\psi'_{4S-3D}\rangle \\ |\psi''_{4S-3D}\rangle \end{pmatrix} = \begin{pmatrix} \cos\theta & \sin\theta \\ -\sin\theta & \cos\theta \end{pmatrix} \begin{pmatrix} |4^3S_1\rangle \\ |3^3D_1\rangle \end{pmatrix}$$

Wang, Chen, XL, TM, PRD99 (2019) 114003

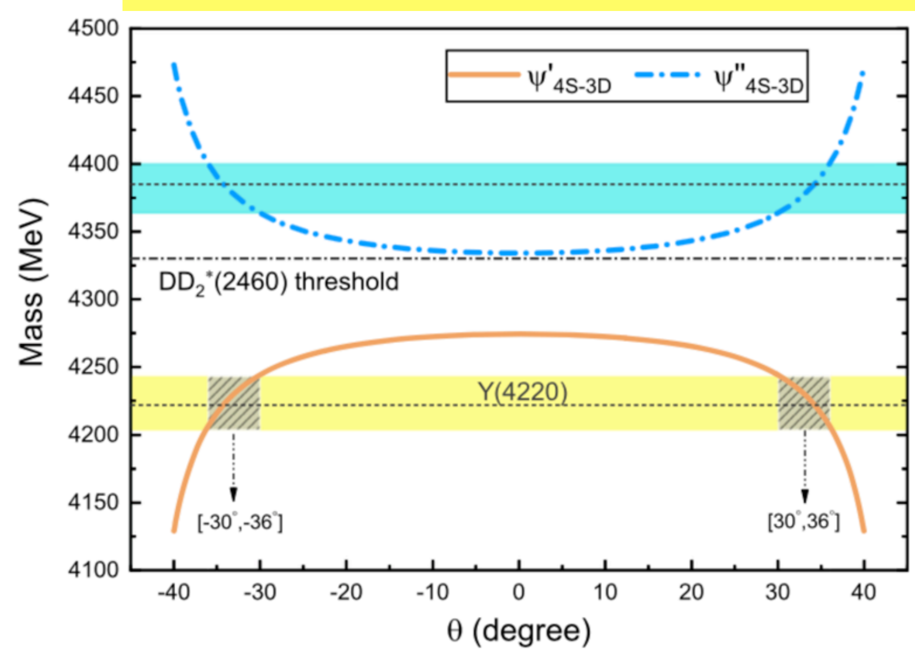


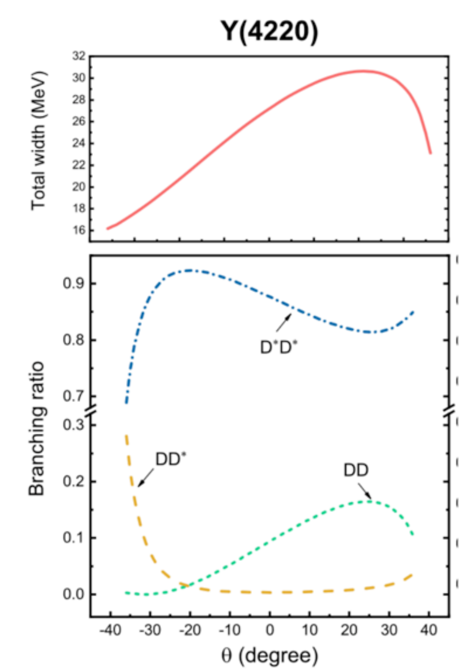


**Our calculation supports this scenario**

21

**Question from the audience: Why is the mixing angle at $\sim 30°$?**

## We seek to address this question within this year

arXiv:2502.08072

### Unraveling charmonium mixing scheme for the $\psi(4220)$ and $\psi(4380)$ by a coupled-channel approach

Zi-Long Man[1,2,3,4], Si-Qiang Luo[1,2,3,4], Zi-Yue Bai[1,2,3,4], and Xiang Liu[1,2,3,4*]
[1]*School of Physical Science and Technology, Lanzhou University, Lanzhou 730000, China*
[2]*Lanzhou Center for Theoretical Physics, Key Laboratory of Theoretical Physics of Gansu Province, Key Laboratory of Quantum Theory and Applications of MoE, Gansu Provincial Research Center for Basic Disciplines of Quantum Physics, Lanzhou University, Lanzhou 730000, China*
[3]*MoE Frontiers Science Center for Rare Isotopes, Lanzhou University, Lanzhou 730000, China*
[4]*Research Center for Hadron and CSR Physics, Lanzhou University and Institute of Modern Physics of CAS, Lanzhou 730000, China*
(Dated: May 2024)

Among charmoniumlike *XYZ* states, the $\psi(4220)$ and $\psi(4380)$ states have emerged as key candidates for exploring the charmonium spectrum. In this work, we propose a $4S$-$3D$ charmonium mixing scheme for the $\psi(4220)$ and $\psi(4380)$, induced by coupled-channel effects. By constructing a coupled-channel model, we identify the dynamical mechanism responsible for the large mixing angle observed in previous studies, which cannot be explained by conventional potential models alone. Our analysis reveals that the $DD_1$ channel significantly influences the lower state ($\psi(4220)$), while the $D^*D_1$ channel primarily affects the higher state ($\psi(4380)$). Furthermore, we investigate the two-body Okubo-Zweig-Iizuka (OZI)-allowed strong decay behaviors of these states, providing insights into their total widths. This study not only supports the $4S$-$3D$ mixing scheme but also offers a deeper understanding of the role of coupled channels in shaping the charmonium spectrum above 4 GeV. Our results align with experimental observations and provide a framework for interpreting future data on charmonium states.

# 2. Mixing scheme for $\psi(4220)$ induced by a coupled-channel approach

$$\underbrace{\begin{pmatrix} M_{4S}^0 & 0 \\ 0 & M_{3D}^0 \end{pmatrix}}_{\text{Bare}} + \underbrace{\begin{pmatrix} 0 & \langle 4S|H_T|3D\rangle \\ \langle 3D|H_T|4S\rangle & 0 \end{pmatrix}}_{\text{Potential model}}$$

$$+ \underbrace{\sum_{BC} \begin{pmatrix} \langle 4S|-\bigcirc_{C}^{B}-|4S\rangle & \langle 4S|-\bigcirc_{C}^{B}-|3D\rangle \\ \langle 3D|-\bigcirc_{C}^{B}-|4S\rangle & \langle 3D|-\bigcirc_{C}^{B}-|3D\rangle \end{pmatrix}}_{\text{Coupled-channel contribution}}$$

The tensor term in the potential model is insufficient to generate large mixing

$$\begin{pmatrix} M_S^0 & \langle\psi_S|H_{\mathrm{T}}|\psi_D\rangle \\ \langle\psi_D|H_{\mathrm{T}}|\psi_S\rangle & M_D^0 \end{pmatrix}\begin{pmatrix} C_S \\ C_D \end{pmatrix} = M\begin{pmatrix} C_S \\ C_D \end{pmatrix}$$

$$H_T = \frac{4\alpha_s}{3m_c m_{\bar c} r^3}\left(\frac{3(\boldsymbol{S}_c\cdot\boldsymbol{r})(\boldsymbol{S}_{\bar c}\cdot\boldsymbol{r})}{r^2} - \boldsymbol{S}_c\cdot\boldsymbol{S}_{\bar c}\right)$$

$$\begin{pmatrix} |\psi'_{4S-3D}\rangle \\ |\psi''_{4S-3D}\rangle \end{pmatrix} = \begin{pmatrix} \cos\theta & \sin\theta \\ -\sin\theta & \cos\theta \end{pmatrix}\begin{pmatrix} |4^3S_1\rangle \\ |3^3D_1\rangle \end{pmatrix}$$

**The coupled-channel effect results in large S-D mixing scheme**

$$\det\begin{vmatrix} M_S^0 + \Delta M_S(M) - M & \langle\psi_S|H_T|\psi_D\rangle + \Delta M_{SD}(M) \\ \langle\psi_D|H_T|\psi_S\rangle + \Delta M_{SD}(M) & M_D^0 + \Delta M_D(M) - M \end{vmatrix} = 0$$

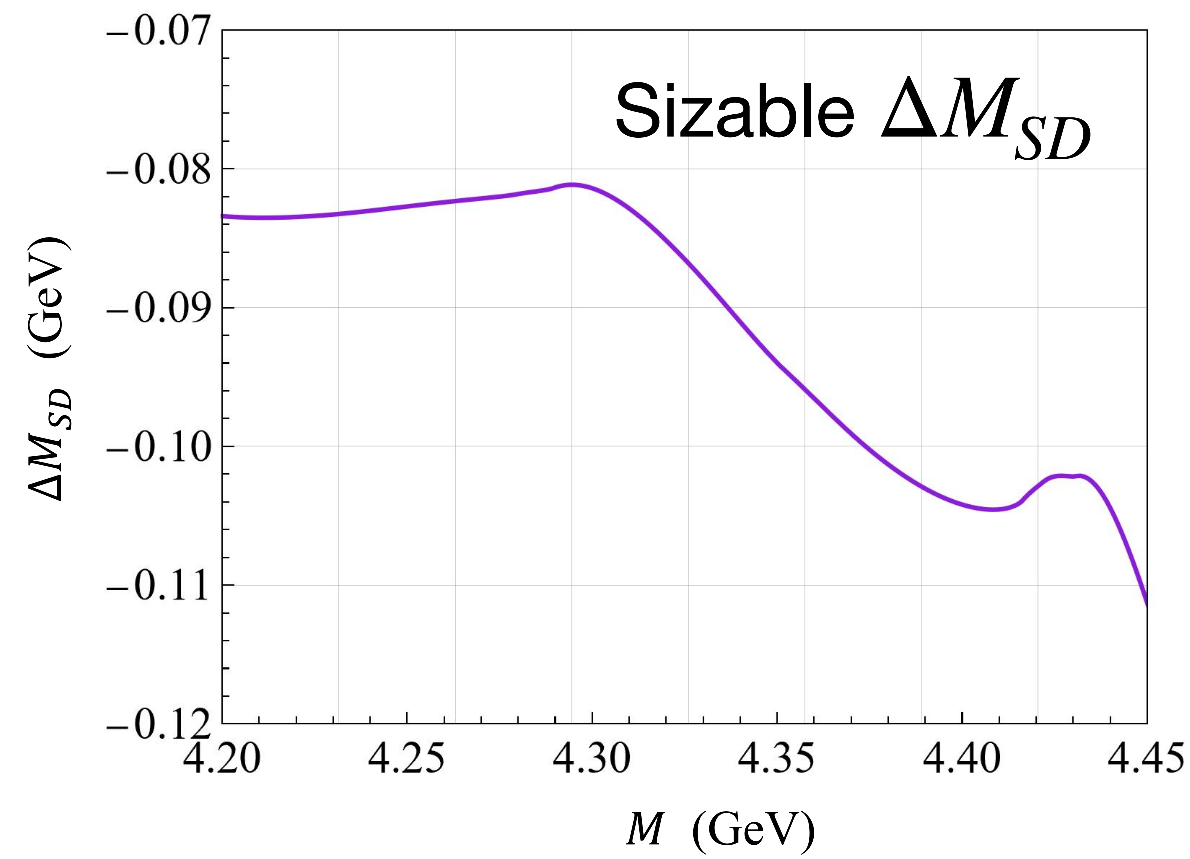


Mixing angle: $\theta = 35^\circ$

见满自龙的会议报告

# 3. Reevaluating the $\psi(4160)$ resonance paramete

The mass changes from 4160 MeV to 4190 MeV

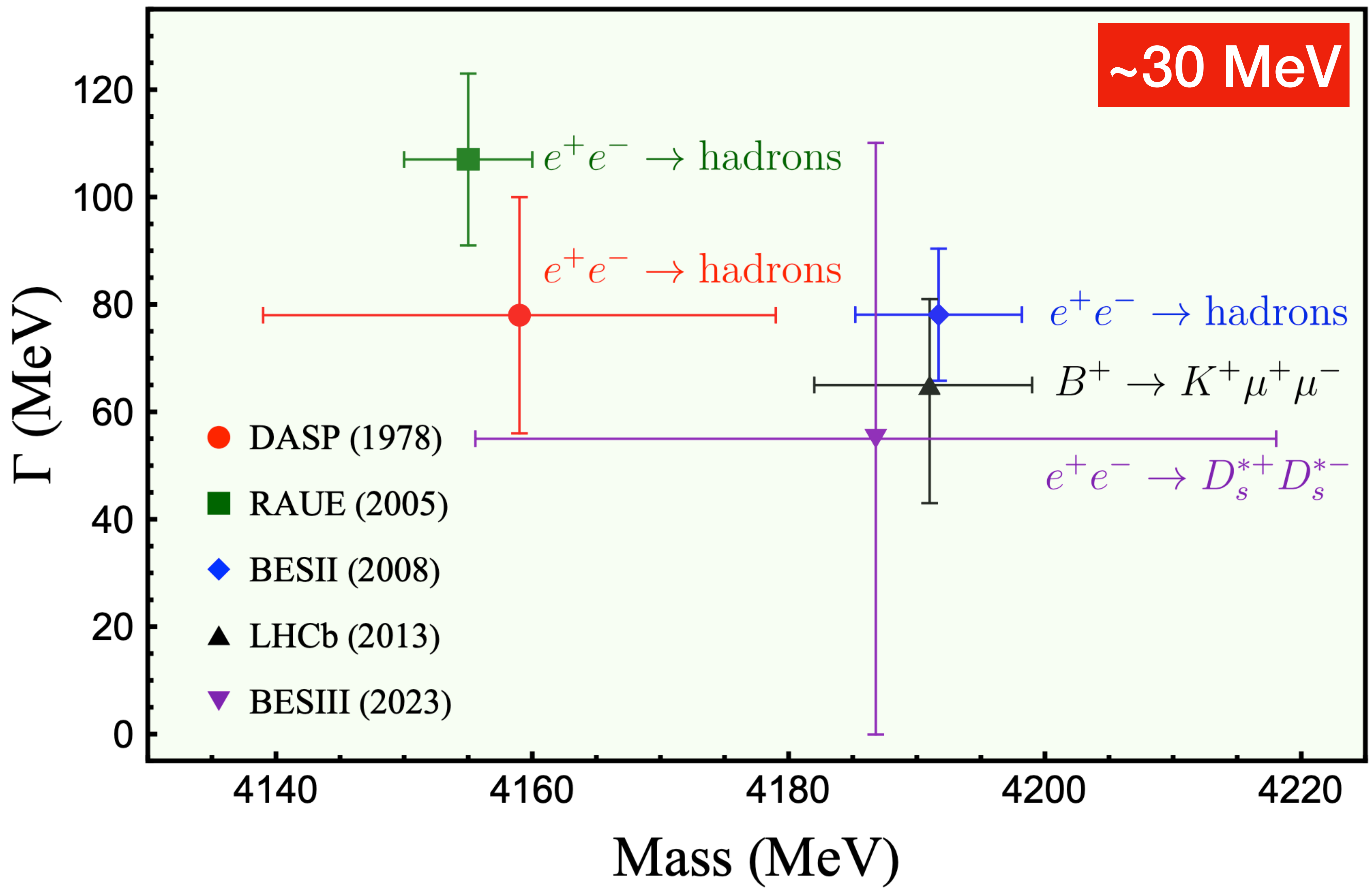

# 3. Reevaluating the $\psi(4160)$ resonance paramete

$$B^+ \to K^+ \boxed{\mu^+\mu^-} \longrightarrow \text{From vector charmonium}$$

The decay process $B^+ \to K^+\mu^+\mu^-$ can occur through three distinct mechanisms, where the dimuon pair ($\mu^+\mu^-$) couples to a $Z^0$ boson, a photon ($\gamma$), or a vector resonance. These contributions are represented by the amplitudes $\mathcal{A}^{\mathrm{AV}}_{\mathrm{nonres}}(Z^0)$, $\mathcal{A}^{\mathrm{V}}_{\mathrm{nonres}}(Z^0 \text{ and } \gamma)$, and $\mathcal{A}^n_{\mathrm{res}}$. The superscripts AV and V are used to denote the first two terms, reflecting the axial-vector (AV) and vector (V) nature of the couplings involved. The total amplitude is

$$\mathcal{A}_{\mathrm{Tot}} = \mathcal{A}^{\mathrm{AV}}_{\mathrm{nonres}} + \mathcal{A}^{\mathrm{V}}_{\mathrm{nonres}} + \sum_n f_n e^{i\delta_n} \mathcal{A}^n_{\mathrm{res}}. \quad (2)$$

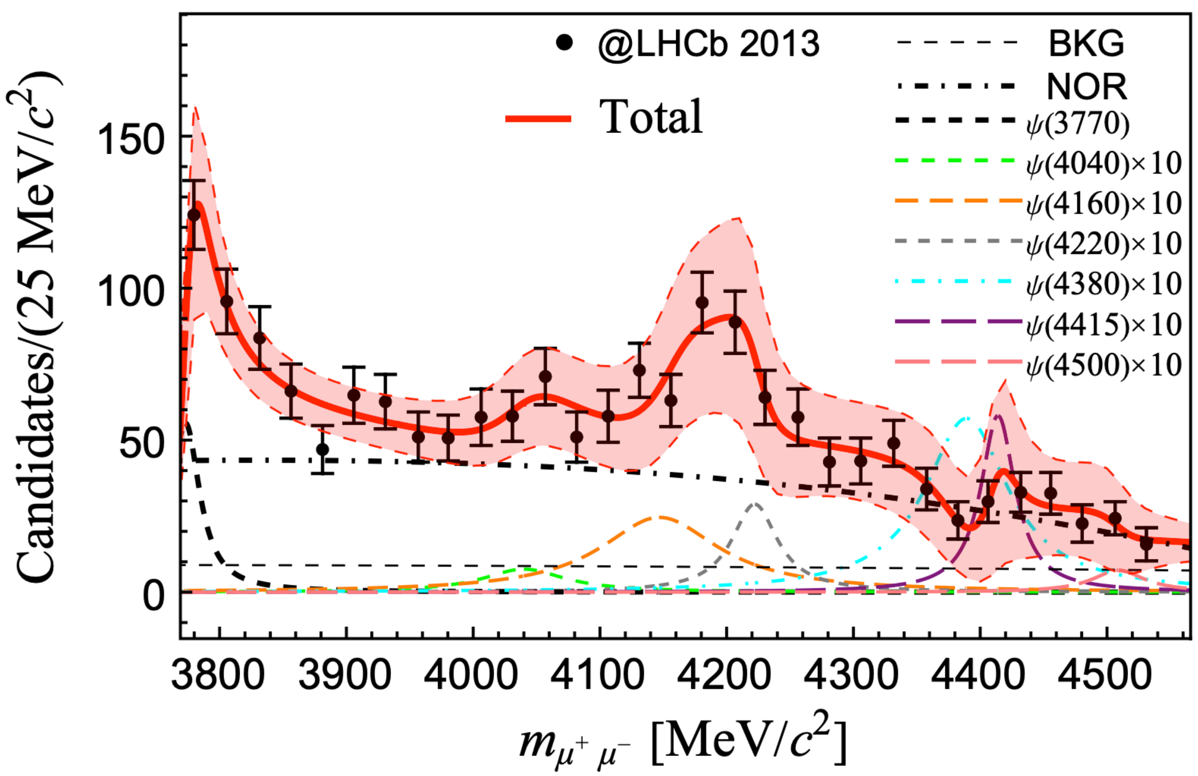


TABLE I. The masses and widths of higher charmonium states in the range of 4.0–4.5 GeV, which were obtained from the theoretical predictions [13–15], as well as some experimental values [3,4].

| States | Mass (MeV) | $\Gamma$ (MeV) |
|---|---|---|
| $\psi(3770)$ | $3773.7 \pm 0.7$ [3] | $27.2 \pm 1.0$ [3] |
| $\psi(4040)$ | $4040 \pm 4$ [3] | $84 \pm 12$ [3] |
| $\psi(4160)$ | $4159 \pm 22$ [4] | $78 \pm 22$ [4] |
| $\psi(4220)$ | 4222 | 44 |
| $\psi(4380)$ | 4389 | 80 |
| $\psi(4415)$ | 4414 | 33 |
| $\psi(4500)$ | 4509 | 50 |

TABLE II. The parameter values obtained from fitting the experimental data are as follows. The factors $f_i$ (in units of MeV) are chosen to ensure that the resonance amplitudes have the same dimensions as the nonresonance contribution. The phases $\delta_i$ (in radians) correspond to the seven $\psi$ states: $\psi(3770)$, $\psi(4040)$, $\psi(4160)$, $\psi(4220)$, $\psi(4380)$, $\psi(4415)$, and $\psi(4500)$, listed in succession.

| Parameters (MeV) | Value | Parameters (rad) | Value |
|---|---|---|---|
| $f_1$ | $46.37 \pm 2.52$ | $\delta_1$ | $0.95 \pm 0.05$ |
| $f_2$ | $4.83 \pm 0.33$ | $\delta_2$ | $2.30 \pm 0.17$ |
| $f_3$ | $7.12 \pm 0.56$ | $\delta_3$ | $1.67 \pm 0.11$ |
| $f_4$ | $8.85 \pm 0.56$ | $\delta_4$ | $4.36 \pm 0.32$ |
| $f_5$ | $9.87 \pm 0.74$ | $\delta_5$ | $5.66 \pm 0.42$ |
| $f_6$ | $9.29 \pm 0.49$ | $\delta_6$ | $2.74 \pm 0.20$ |
| $f_7$ | $3.57 \pm 0.26$ | $\delta_7$ | $5.00 \pm 0.30$ |
| | $\chi^2/\mathrm{d.o.f.} = 0.90$ | | |

# 3. Reevaluating the $\psi(4160)$ resonance paramete

Peng, Bai, Wang, XL, PRD 111 (2025) 054023

A puzzling phenomenon, where the measured mass of the $\psi(4160)$ is pushed higher, presents a challenge to current theoretical models of hadron spectroscopy. This study suggests that the issue arises from analyses based on the outdated quenched charmonium spectrum. In the past two decades, the discovery of new hadronic states has emphasized the importance of the unquenched effect. Under the unquenched picture, six vector charmonium states—$\psi(4040)$, $\psi(4160)$, $\psi(4220)$, $\psi(4380)$, $\psi(4415)$, and $\psi(4500)$—are identified in the 4–4.5 GeV range, contrasting with the three states predicted in the quenched model. We reevaluate the resonance parameters of the $\psi(4160)$ using the dimuon invariant mass spectrum of $B^+ \to K^+\mu^+\mu^-$ and unquenched charmonium spectroscopy. Our analysis indicates previous experimental overestimations for the mass of the $\psi(4160)$. This conclusion is supported by analyzing $e^+e^- \to D_s\bar{D}_s^*$, which finds the $\psi(4160)$ mass at $4145.76 \pm 4.48$ MeV. Our findings have significant implications for both hadron spectroscopy and search for new physics signals by $R_K$.

DOI: 10.1103/PhysRevD.111.054023

## References for unquenched results


- L. P. He, D. Y. Chen, X. Liu, and T. Matsuki, Prediction of a missing higher charmonium around 4.26 GeV in $J/\psi$ family, Eur. Phys. J. C **74**, 3208 (2014).
- D. Y. Chen, X. Liu, and T. Matsuki, Observation of $e^+e^- \to \chi_{c0}\omega$ and missing higher charmonium $\psi(4S)$, Phys. Rev. D **91**, 094023 (2015).
- D. Y. Chen, X. Liu, and T. Matsuki, Search for missing $\psi(4S)$ in the $e^+e^- \to \pi^+\pi^-\psi(2S)$ process, Phys. Rev. D **93**, 034028 (2016).
- D. Y. Chen, X. Liu, and T. Matsuki, Interference effect as resonance killer of newly observed charmoniumlike states $Y(4320)$ and $Y(4390)$, Eur. Phys. J. C **78**, 136 (2018).
- J. Z. Wang, D. Y. Chen, X. Liu, and T. Matsuki, Constructing $J/\psi$ family with updated data of charmoniumlike $Y$ states, Phys. Rev. D **99**, 114003 (2019).
- J. Z. Wang and X. Liu, Confirming the existence of a new higher charmonium $\psi(4500)$ by the newly released data of $e^+e^- \to K^+K^-J/\psi$, Phys. Rev. D **107**, 054016 (2023).
- J. Z. Wang and X. Liu, Identifying a characterized energy level structure of higher charmonium well matched to the peak structures in $e^+e^- \to \pi^+D^0D^{*-}$, Phys. Lett. B **849**, 138456 (2024).
- T. C. Peng, Z. Y. Bai, J. Z. Wang, and X. Liu, How higher charmonia shape the puzzling data of the $e^+e^- \to \eta J/\psi$ cross section, Phys. Rev. D **109**, 094048 (2024).


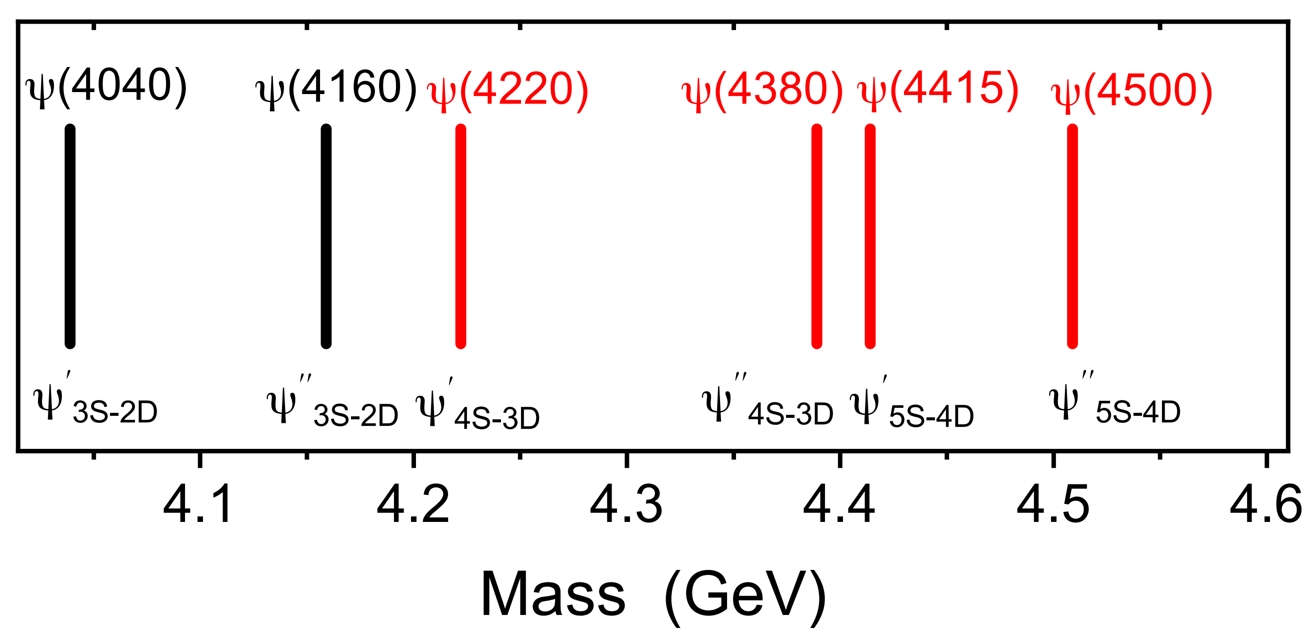

# 3. Reevaluating the $\psi(4160)$ resonance paramete

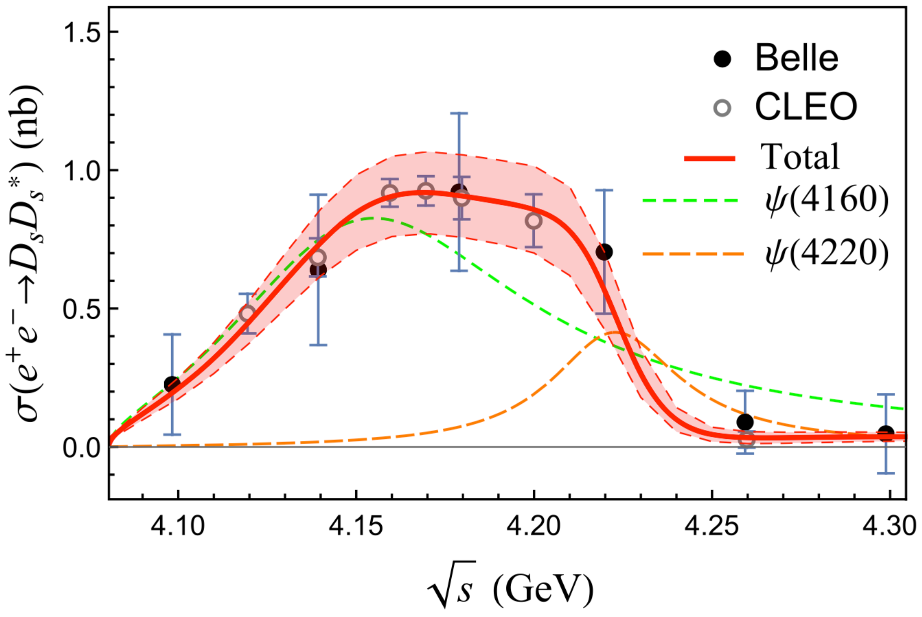


FIG. 3. The black and hollow dots with error bands represent the experimental data from the Belle and CLEO Collaborations [28,29], respectively. The dashed lines show the individual contributions from the $\psi(4160)$ and $\psi(4220)$ resonances. The red curve with a band represents the total contribution and uncertainties.

$$\psi(4160) + \psi(4220)$$

$$\sigma(s) = |\mathrm{BW}_1(s) + \mathrm{BW}_2(s)e^{i\phi}|^2,$$

$$\mathrm{BW}(s) = \frac{\sqrt{12\pi\Gamma_\psi^{ee}\Gamma_{\mathrm{tot}}\mathcal{B}(\psi\to D_s\bar{D}_s^*)}}{s-M^2+iM\Gamma_{\mathrm{R}}}\sqrt{\frac{\mathrm{PS}(\sqrt{s})}{\mathrm{PS}(M)}},$$

Peng, Bai, Wang, XL, PRD 111 (2025) 054023

TABLE III. The fitting parameters $m_{\psi(4160)}$, $\Gamma_{\psi(4160)}$, $\Gamma_\psi^{ee}$, and $\mathcal{B}_\psi$ represent mass, total width, dilepton width, and branch ratio of $\psi\to D_s\bar{D}_s^*$, respectively, and $\phi$(rad) is the phase between the resonance amplitudes associated with the $\psi(4160)$ and $\psi(4220)$ in the $e^+e^-\to D_s\bar{D}_s^*$ cross section.

| Parameters | Best fit | I | II | III | IV |
|---|---|---|---|---|---|
| $m_{\psi(4160)}$ (MeV) | $\boxed{4145.76 \pm 5.48}$ | 4140 (fixed) | 4150 (fixed) | 4160 (fixed) | 4170 (fixed) |
| $\Gamma_{\psi(4160)}$ (MeV) | $\boxed{104.83 \pm 23.71}$ | $113.98 \pm 24.01$ | $108.78 \pm 23.65$ | $127.17 \pm 17.65$ | $143.37 \pm 25.24$ |
| $\Gamma^{ee}_{\psi(4160)}\mathcal{B}_{\psi(4160)}$ (eV) | $98.02 \pm 26.88$ | $108.43 \pm 29.8$ | $109.14 \pm 30.04$ | $168.42 \pm 35.09$ | $207.29 \pm 25.91$ |
| $\Gamma^{ee}_{\psi(4220)}\mathcal{B}_{\psi(4220)}$ (eV) | $22.09 \pm 8.82$ | $23.23 \pm 10.00$ | $21.32 \pm 10.96$ | $51.12 \pm 34.72$ | $66.81 \pm 22.22$ |
| $\phi$ (rad) | $2.91 \pm 0.27$ | $2.90 \pm 0.23$ | $3.01 \pm 0.30$ | $3.35 \pm 0.23$ | $3.25 \pm 0.14$ |
| $\chi^2$/d.o.f. | 0.22 | 0.31 | 0.26 | 0.79 | 1.88 |

# 4. Discovery potential of charmonium 2P states through $e^+e^- \to \omega D\bar{D}$ and $e^+e^- \to \gamma D\bar{D}$

## 2P charmonia:

$X(3915) \equiv \chi_{c0}(2P)$

$X(3872) \equiv \chi_{c1}(2P)$

$Z(3930) \equiv \chi_{c2}(2P)$

LHCb, PRD 102 (2020) 112003

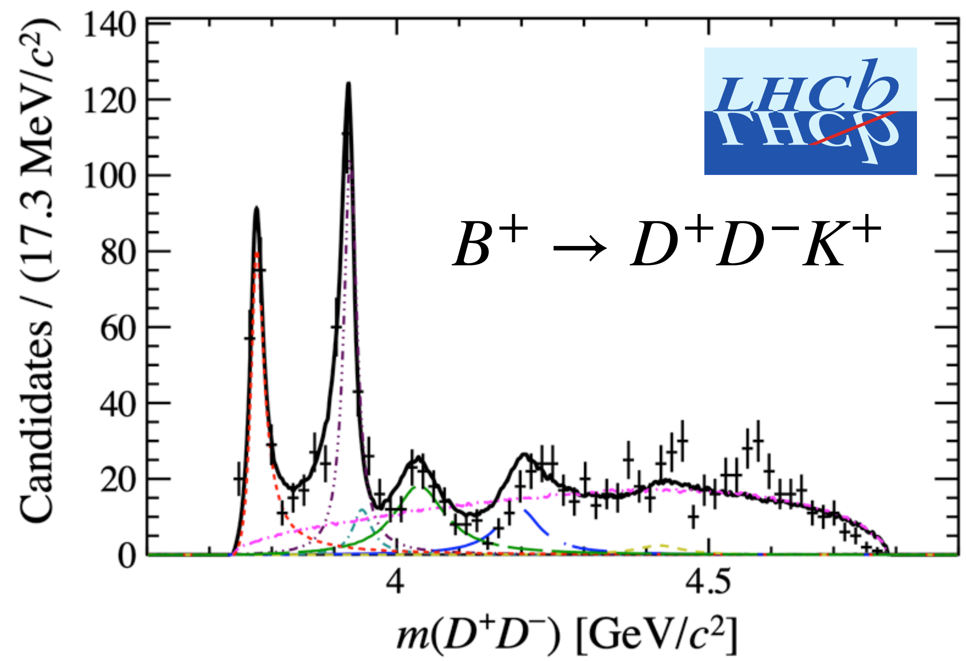


XL, Sun, Luo, PRL 104 (2010) 122001

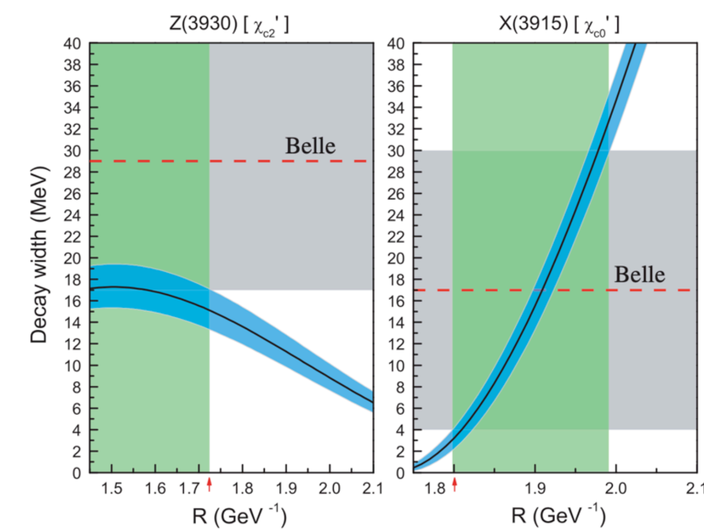


FIG. 2 (color online). The dependence of the decay width of $Z(3930)$ and $X(3915)$ on $R$ under $\chi_{c2}'$ and $\chi_{c0}'$ assignment for $Z(3930)$ and $X(3915)$, respectively. Here, red dashed lines with grey bands denote the central value for the error of total width of $X(3915)$ and $Z(3930)$ measured by Belle [1,3]. The green bands denote the regions of $R$ resulting in the theoretical values consistent with Belle data. The solid lines with blue error bands are our calculation result.

Belle, PRL 104 (2010) 092001

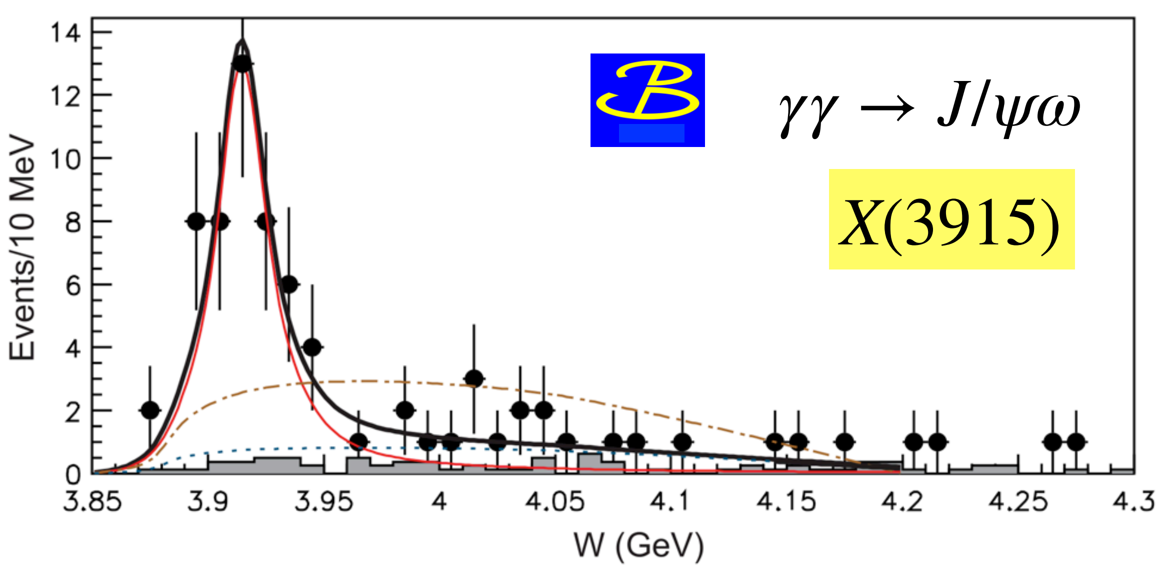


Belle, PRL 96 (2006) 082003

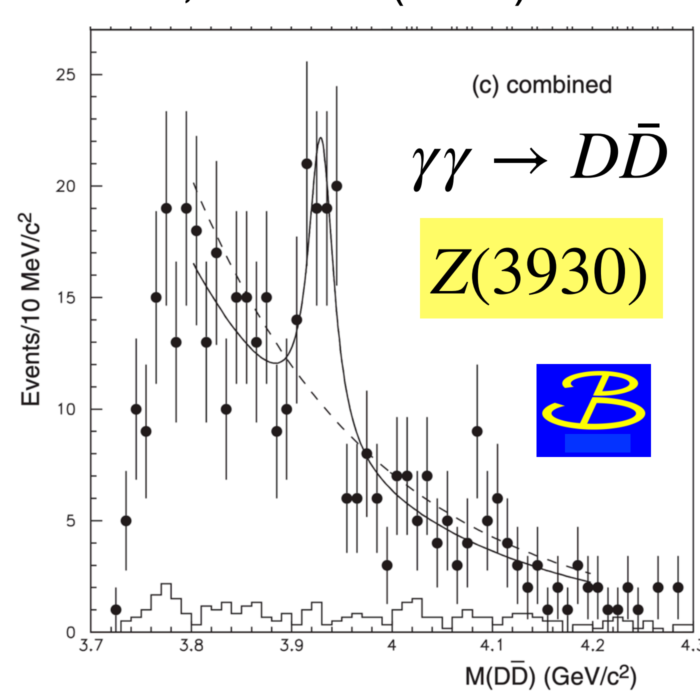


### Relevant work involved in this issue

D.-Y. Chen, J. He, X. Liu, T. Matsuki, and T. Matsuki, Does the enhancement observed in $\gamma\gamma \to D\bar{D}$ contain two $P$-wave higher charmonia?, Eur. Phys. J. C **72**, 2226 (2012).

D.-Y. Chen, X. Liu, and T. Matsuki, Hidden-charm decays of $X(3915)$ and $Z(3930)$ as the P-wave charmonia, Prog. Theor. Exp. Phys. **2015**, 43B05 (2015).

M.-X. Duan, J.-Z. Wang, Y.-S. Li, and X. Liu, Role of the newly measured $B \to KD\bar{D}$ process to establish $\chi_{c0}(2P)$ state, Phys. Rev. D **104**, 034035 (2021).

$D\bar{D}$ channel is important to identify $\chi_{c0}(2P)$ and $\chi_{c2}(2P)$

# 4. Discovery potential of charmonium 2P states through $e^+e^- \to \omega D\bar{D}$ and $e^+e^- \to \gamma D\bar{D}$

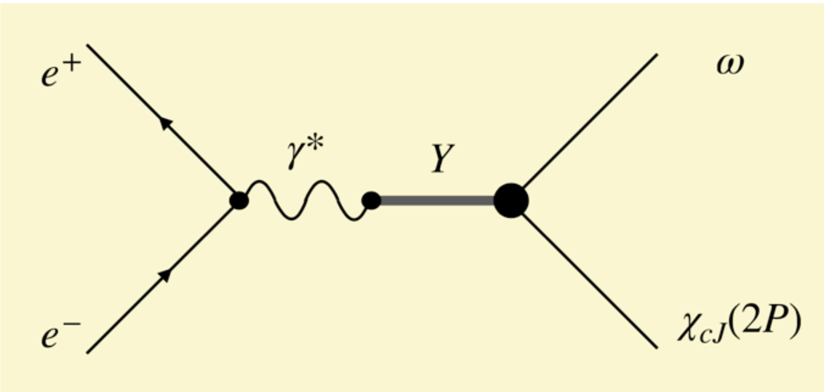


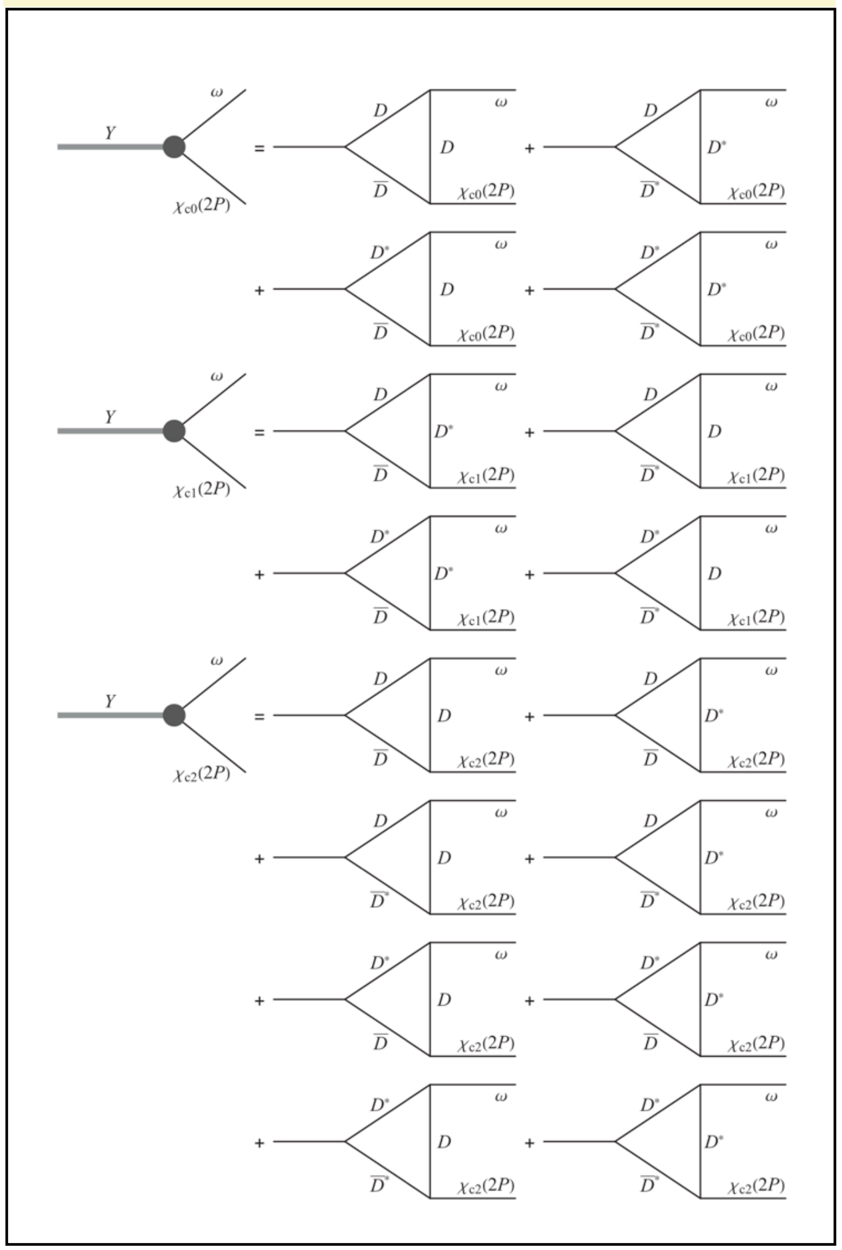

$$
\begin{aligned}
\mathcal{M}^{(a)}_{\omega\chi_{c1}} = i^3 \int & \frac{d^4q}{(2\pi)^4}\frac{1}{q_1^2-m_D^2}\frac{1}{q_2^2-m_D^2}\frac{-g^{\delta\gamma}+q^\delta q^\gamma/m_{D^*}^2}{q^2-m_{D^*}^2} \\
& \times[-g_{\psi DD}\epsilon_\psi^\mu(q_{1\mu}-q_{2\mu})] \\
& \times[-2f_{DD^*\omega}\epsilon_{\nu\kappa\delta\sigma}\epsilon_\omega^{*\nu}p_k^\kappa(q_1^\sigma+q^\sigma)] \\
& \times[-ig_{\chi_{c1}DD^*}\epsilon^{*\theta}_{\chi_{c1}}g_{\theta\gamma}]\underline{\mathcal{F}^2(q^2)},
\end{aligned}
$$

$$
\boxed{\mathcal{F}(q^2) = \left(\frac{m_E^2-\Lambda^2}{q^2-\Lambda^2}\right)^2}
$$

**Suggest BESIII to focus on this issue**

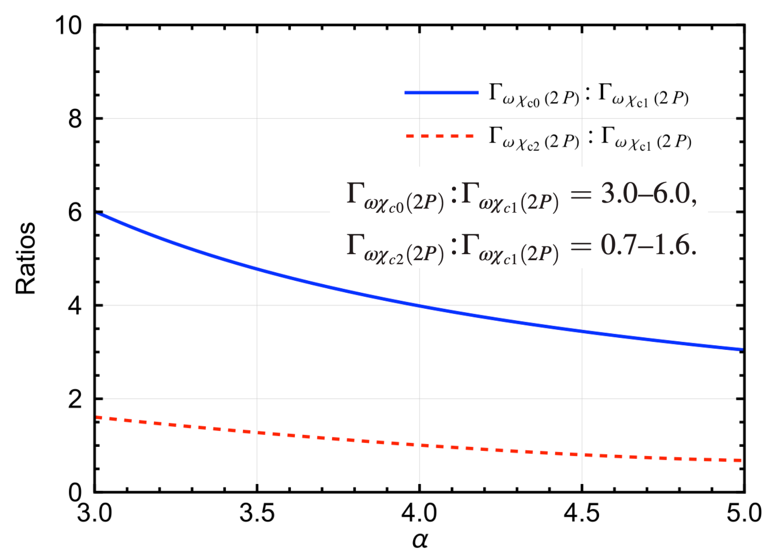


FIG. 3. The dependence of the ratios of partial widths of three decay channels $Y \to \omega\chi_{cJ}(2P)$ on $\alpha$.

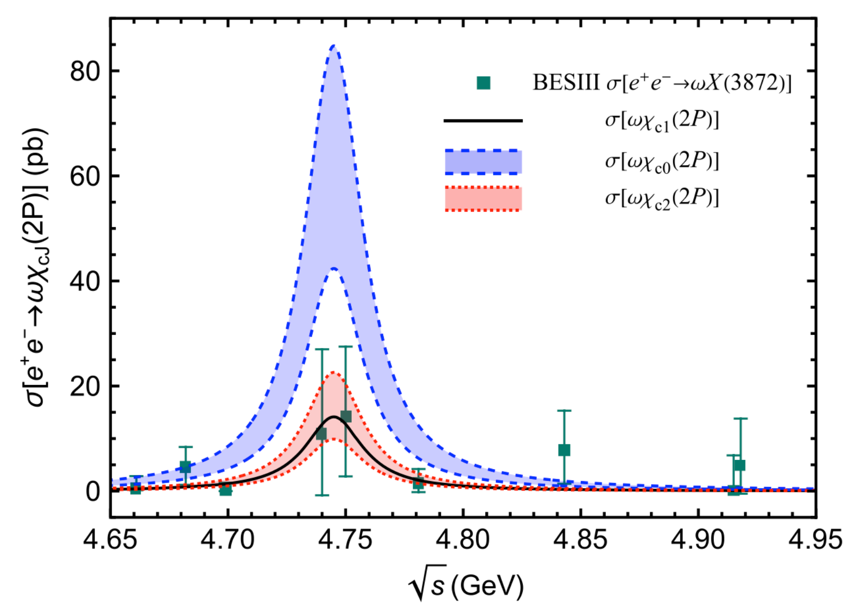


FIG. 4. The predicted cross sections of $e^+e^- \to \omega\chi_{c0}(2P)$ and $e^+e^- \to \omega\chi_{c2}(2P)$. Here, we take the experimental data of $e^+e^- \to \omega X(3872)$ [1] as the scaling point, treating $X(3872) \equiv \chi_{c1}(2P)$.

# 4. Discovery potential of charmonium 2P states through $e^+e^- \to \omega D\bar{D}$ and $e^+e^- \to \gamma D\bar{D}$

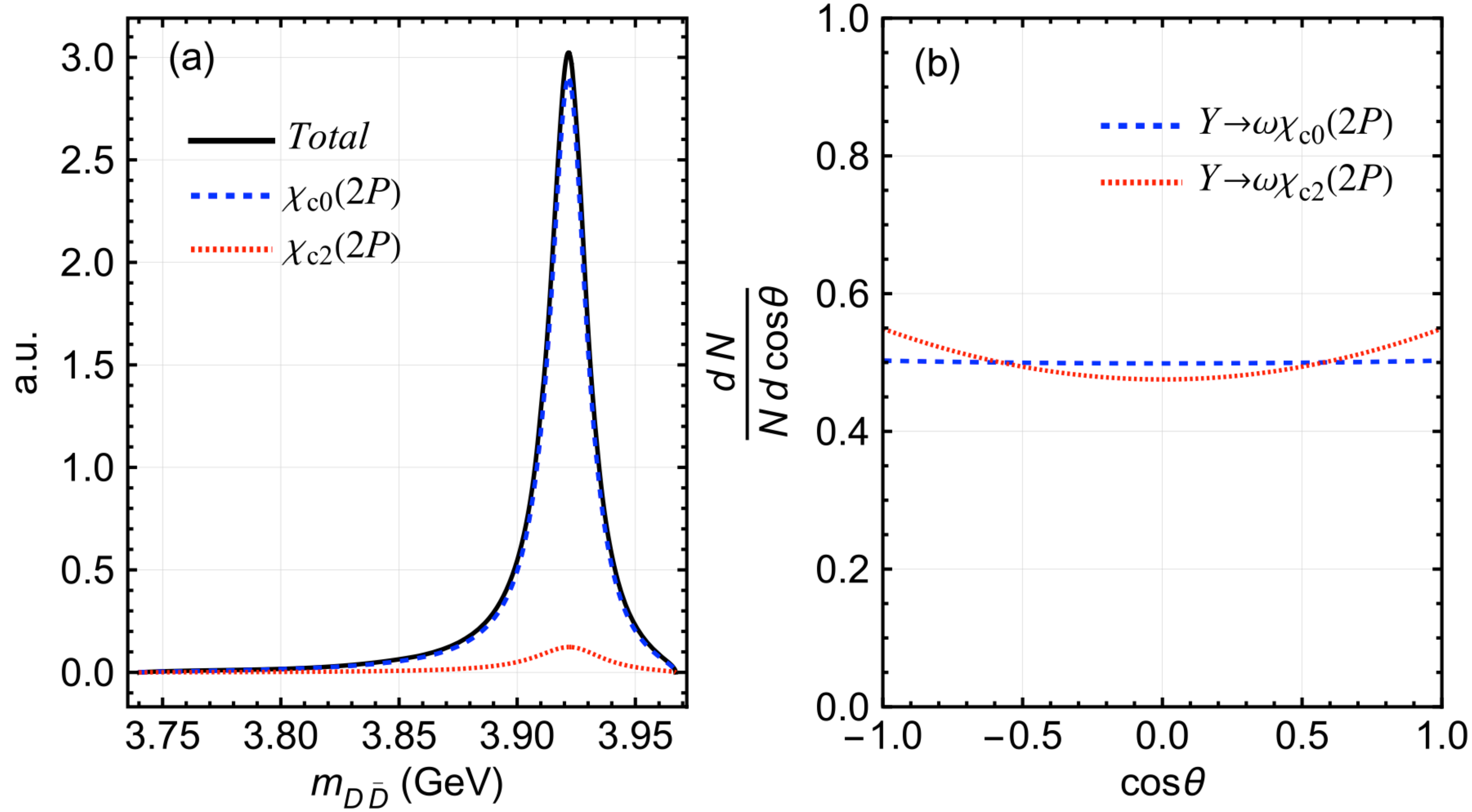


FIG. 5. (a) The predicted invariant mass spectrum of $D\bar{D}$ of $e^+e^- \to \omega D\bar{D}$. (b) The calculated angular distributions of $Y \to \omega\chi_{c0,2}(2P)$. Here, the results are properly normalized.

Qian, XL, PRD 108 (2023) 094046

# 4. Discovery potential of charmonium 2P states through $e^+e^- \to \omega D\bar{D}$ and $e^+e^- \to \gamma D\bar{D}$

Gao, Qian, XL, PRD 111 (2025) 054021

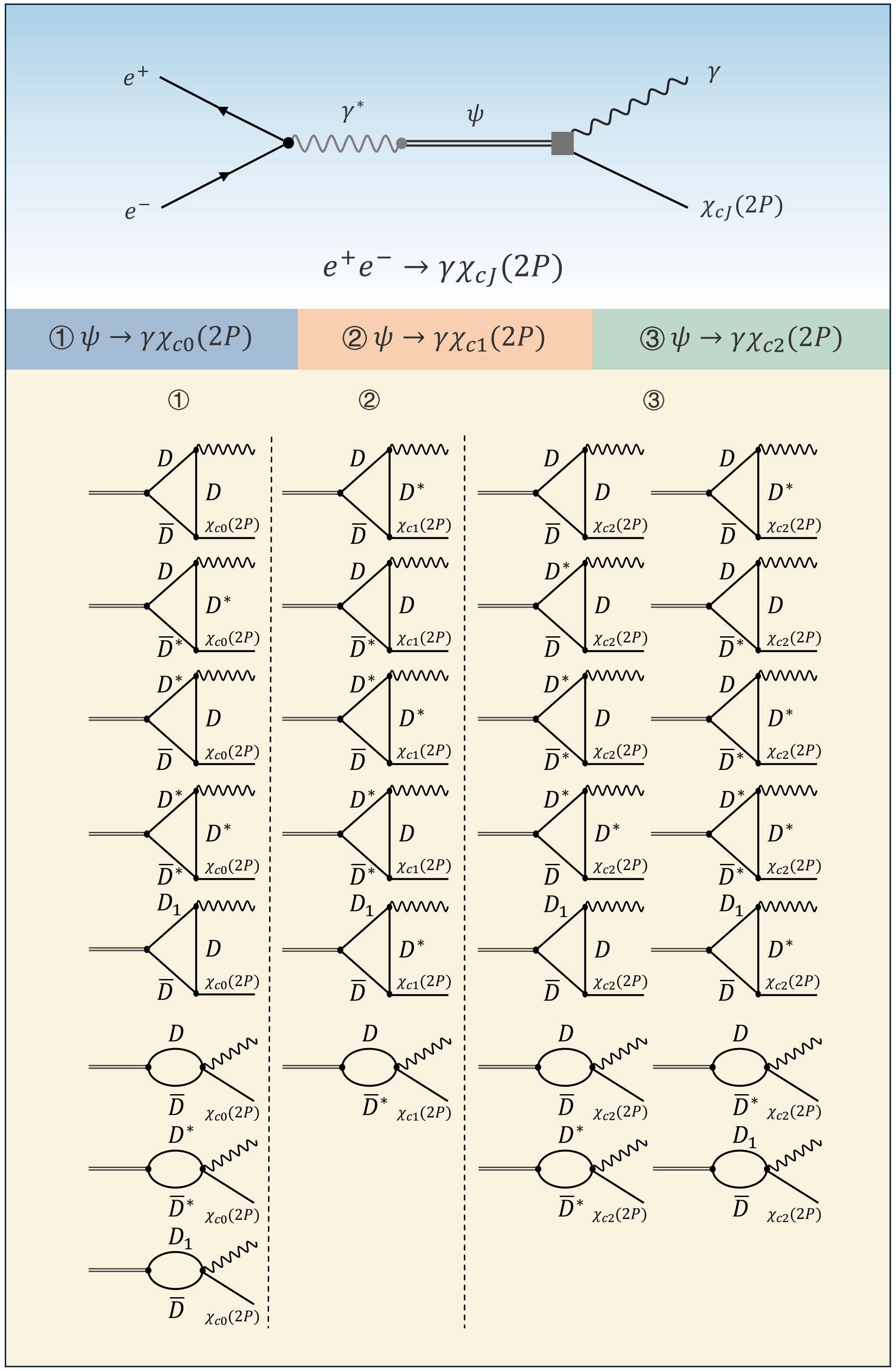


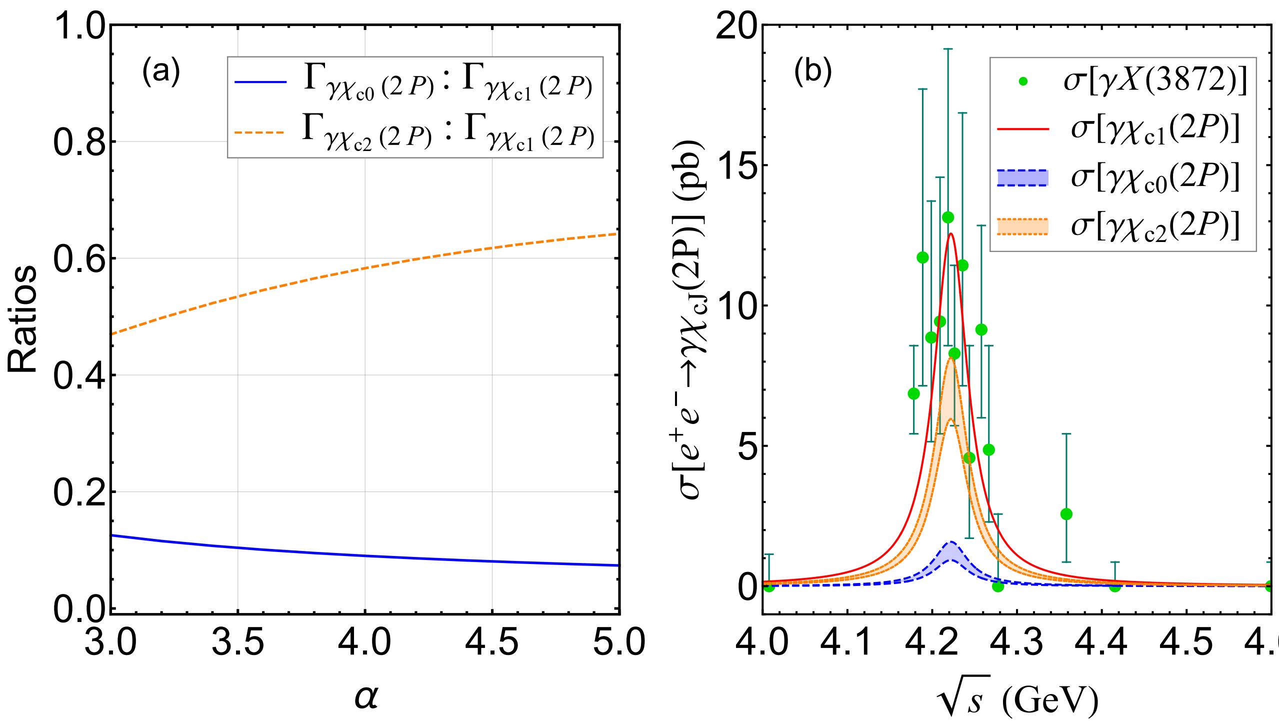


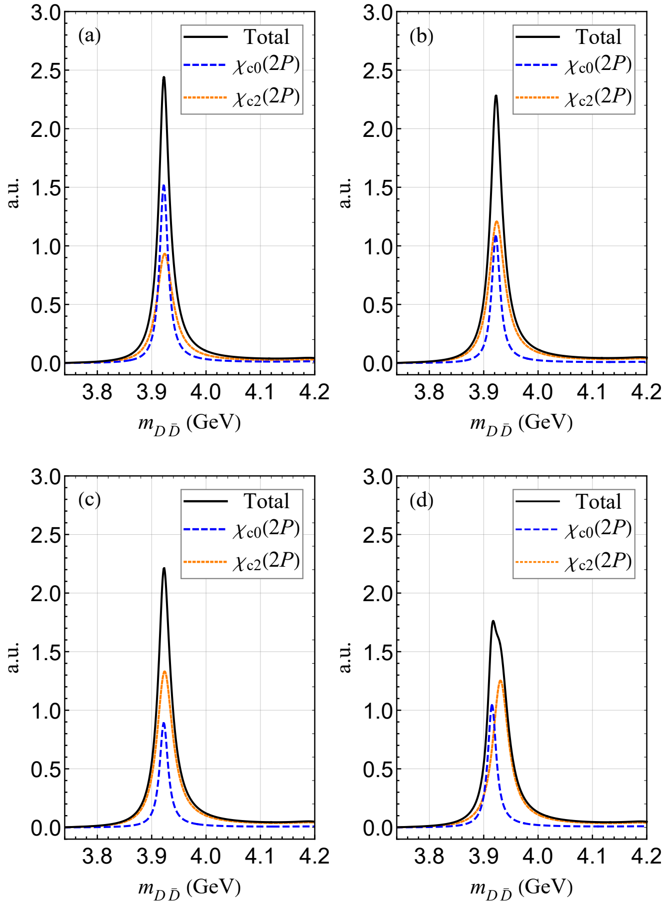


Our results indicate that $e^+e^- \to \gamma D\bar{D}$ is ideal process to study 2P states of charmonium

# Non-$D\bar{D}$ decay of $\psi(3770)$ is sizable

Citation: S. Navas *et al.* (Particle Data Group), Phys. Rev. D **110**, 030001 (2024)

$\boxed{\psi(3770)}$ $\qquad I^G(J^{PC}) = 0^-(1^{--})$

## $\psi(3770)$ BRANCHING RATIOS

$\Gamma(D\overline{D})/\Gamma_{\text{total}}$ $\qquad \Gamma_1/\Gamma = (\Gamma_2+\Gamma_3)/\Gamma$

| *VALUE* | *EVTS* | *DOCUMENT ID* | | *TECN* | *COMMENT* |
|---|---|---|---|---|---|
| $\boxed{\mathbf{0.93^{+0.08}_{-0.09}}}$ | **OUR FIT** Error includes scale factor of 2.0. | | | | |
| $\mathbf{0.93^{+0.08}_{-0.09}}$ | **OUR AVERAGE** Error includes scale factor of 2.1. | | | | |
| $0.849\pm0.056\pm0.018$ | | [1] ABLIKIM | 08B | BES2 | $e^+e^- \to$ non-$D\overline{D}$ |
| $1.033\pm0.014^{+0.048}_{-0.066}$ | 1.427M | [2] BESSON | 06 | CLEO | $e^+e^- \to$ hadrons |
| • • • We do not use the following data for averages, fits, limits, etc. • • • | | | | | |
| $0.836\pm0.049$ | | [3] SHAMOV | 17 | RVUE | $e^+e^- \to D\overline{D}$, hadrons |
| $0.866\pm0.050\pm0.036$ | | [4,5] ABLIKIM | 07K | BES2 | $e^+e^- \to$ non-$D\overline{D}$ |
| $0.836\pm0.073\pm0.042$ | | [5] ABLIKIM | 06L | BES2 | $e^+e^- \to D\overline{D}$ |
| $0.855\pm0.017\pm0.058$ | | [5,6] ABLIKIM | 06N | BES2 | $e^+e^- \to D\overline{D}$ |

# 5. Non-$D\bar{D}$ decays of $\psi_3(3842)$

**1D charmonia:**

$\psi(1^{--}) \equiv \psi(3770)$

$\psi_2(2^{--}) \equiv \psi_2(3823)$

$\psi_2(2^{-+})$

$\psi_3(3^{--}) = \psi_3(3842)$

LHCb, JHEP 07 (2019) 035

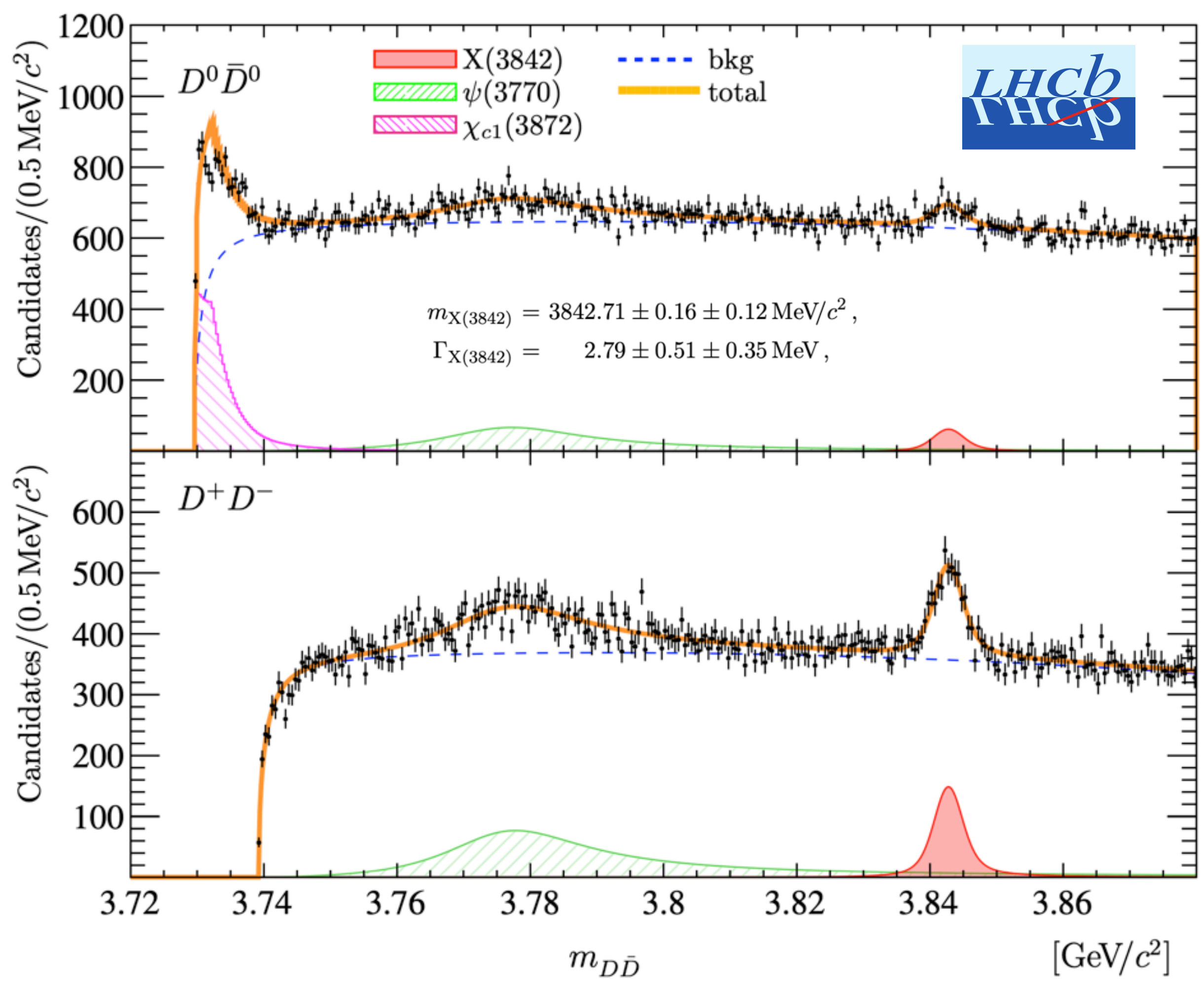


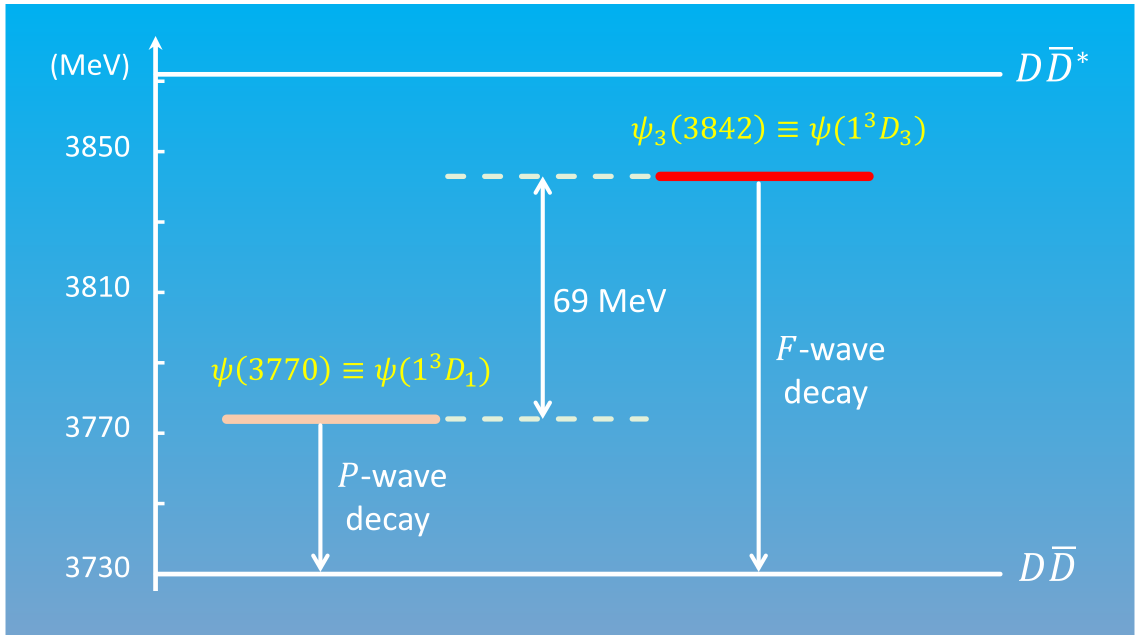


- $\psi(3770)$ dominantly decays into $D\bar{D}$ via P-wave
- $\psi_3(3842)$ dominantly decays into $D\bar{D}$ via F-wave
- We have reason to conjecture that there exists sizable non-$D\bar{D}$ decay

# 5. Non-$D\bar{D}$ decays of $\psi_3(3842)$

## Non-$D\bar{D}$ decay of $\psi_3(3842)$ occurs via hadronic loop

TABLE I: The detailed intermediate loops connecting the initial state $\psi_3(3842)$ to the final states of $PP$, $PV$, and $VV$ as depicted in Fig. 2.

| Final states | | | Hadronic loops |
|---|---|---|---|
| $PP$ | $K\bar{K}$ | $\bar{K}^0(p_1)K^0(p_2)$ | $D^+(q_1)D^-(q_2)D_s^{*+}(q)$ |
| | | $K^-(p_1)K^+(p_2)$ | $D^0(q_1)\bar{D}^0(q_2)D_s^{*+}(q)$ |
| $PV$ | $\omega\eta^{(\prime)}$ | $\eta^{(\prime)}(p_1)\omega(p_2)$ | $D^0(q_1)\bar{D}^0(q_2)D^{*0}(q)$ |
| | | | $\bar{D}^0(q_1)D^0(q_2)\bar{D}^{*0}(q)$ |
| | | | $D^+(q_1)D^-(q_2)D^{*+}(q)$ |
| | | | $D^-(q_1)D^+(q_2)D^{*-}(q)$ |
| | $\rho\pi$ | $\pi^0(p_1)\rho^0(p_2)$ | $D^0(q_1)\bar{D}^0(q_2)D^{*0}(q)$ |
| | | | $\bar{D}^0(q_1)D^0(q_2)\bar{D}^{*0}(q)$ |
| | | | $D^+(q_1)D^-(q_2)D^{*+}(q)$ |
| | | | $D^-(q_1)D^+(q_2)D^{*-}(q)$ |
| | | $\pi^-(p_1)\rho^+(p_2)$ | $D^-(q_1)D^+(q_2)\bar{D}^{*0}(q)$ |
| | | | $D^0(q_1)\bar{D}^0(q_2)D^{*+}(q)$ |
| | | $\pi^+(p_1)\rho^-(p_2)$ | $D^+(q_1)D^-(q_2)D^{*0}(q)$ |
| | | | $\bar{D}^0(q_1)D^0(q_2)\bar{D}^{*-}(q)$ |
| | $K\bar{K}^*$ | $K^0(p_1)\bar{K}^{*0}(p_2)$ | $D^-(q_1)D^+(q_2)D_s^{*-}(q)$ |
| | | $\bar{K}^0(p_1)K^{*0}(p_2)$ | $D^+(q_1)D^-(q_2)D_s^{*+}(q)$ |
| | | $K^+(p_1)K^{*-}(p_2)$ | $\bar{D}^0(q_1)D^0(q_2)D_s^{*-}(q)$ |
| | | $K^-(p_1)K^{*+}(p_2)$ | $D^0(q_1)\bar{D}^0(q_2)D_s^{*+}(q)$ |
| $VV$ | $K^*\bar{K}^*$ | $\bar{K}^{*0}(p_1)K^{*0}(p_2)$ | $D^+(q_1)D^-(q_2)D_s^+(q)$ |
| | | | $D^+(q_1)D^-(q_2)D_s^{*+}(q)$ |
| | | $K^{*-}(p_1)K^{*+}(p_2)$ | $D^0(q_1)\bar{D}^0(q_2)D_s^+(q)$ |
| | | | $D^0(q_1)\bar{D}^0(q_2)D_s^{*+}(q)$ |

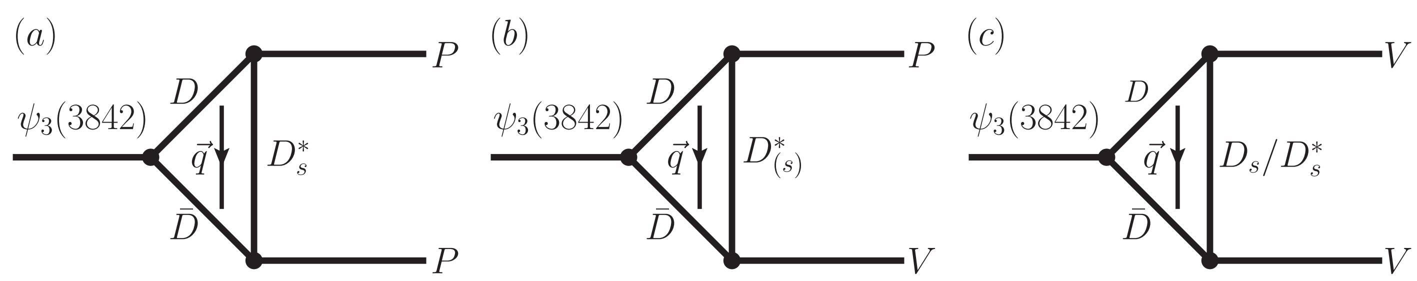


$$\mathcal{M} = \int \frac{d^4 q}{(2\pi)^4} \frac{\mathcal{V}_1 \mathcal{V}_2 \mathcal{V}_3}{\mathcal{P}_1 \mathcal{P}_2 \mathcal{P}_E} \mathcal{F}^2(q^2, m_E^2), \qquad (1)$$

where $\mathcal{P}_i$ ($i = 1, 2, E$) represent the propagators of the intermediate $D_{(s)}^{(*)}$ mesons, and the dipole form factor is given by

$$\mathcal{F}(q^2, m_E^2) = \left( \frac{m_E^2 - \Lambda^2}{q^2 - \Lambda^2} \right)^2 . \qquad (2)$$

$$\Gamma = \frac{1}{7} \frac{|\vec{p}_1|}{8\pi m^2_{\psi_3(3842)}} \sum_{spin} \left| \mathcal{M}^{\mathrm{Total}} \right|^2,$$

# 5. Non-$D\bar{D}$ decays of $\psi_3(3842)$

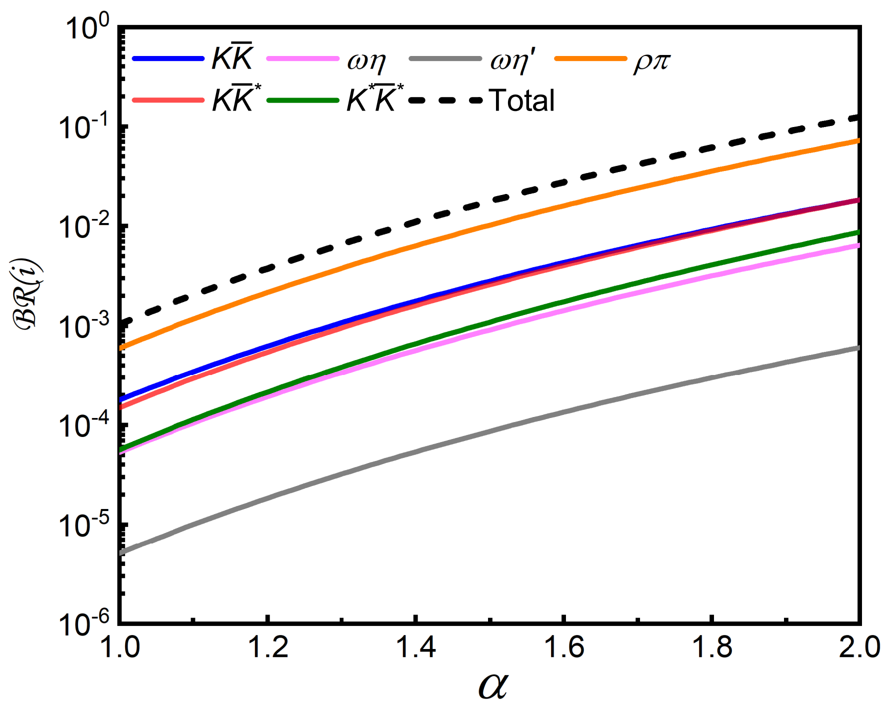


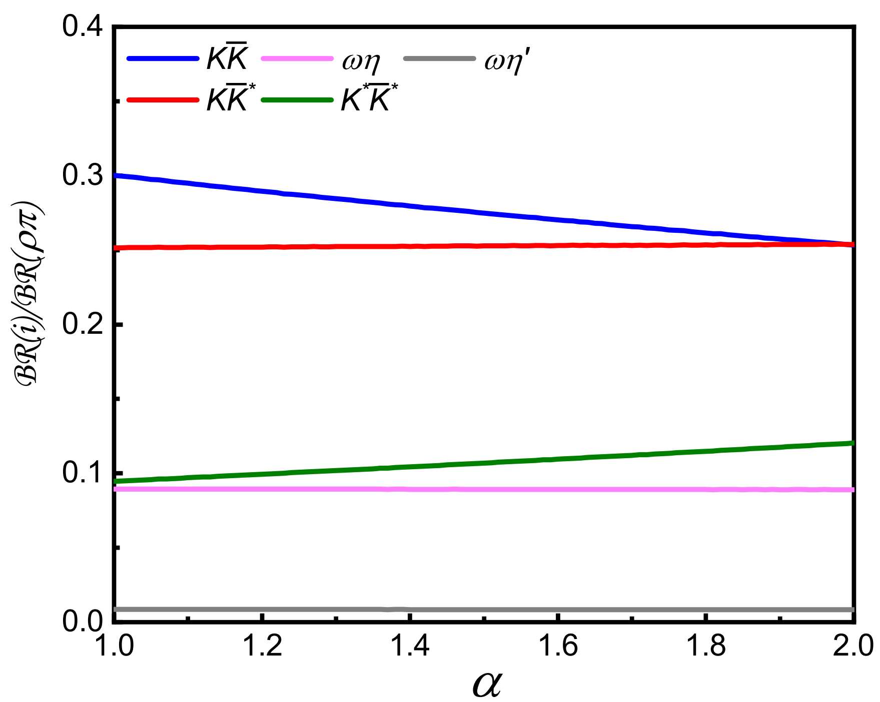


TABLE II: The branching ratios ($\mathcal{BR}$) of $\psi_3(3842)$ decays into allowed $PP$, $PV$, and $VV$ final states for specific values of the $\alpha$ parameter.

| $\mathcal{BR}$ (%) | $\alpha = 1.00$ | $\alpha = 1.25$ | $\alpha = 1.50$ | $\alpha = 1.75$ | $\alpha = 2.00$ |
|---|---|---|---|---|---|
| $K\bar{K}$ | 0.02 | 0.08 | 0.28 | 0.77 | 1.83 |
| $\omega\eta$ | 0.01 | 0.03 | 0.09 | 0.26 | 0.64 |
| $\omega\eta'$ | 0 | 0 | 0.01 | 0.02 | 0.06 |
| $\rho\pi$ | 0.06 | 0.29 | 1.02 | 2.93 | 7.21 |
| $K\bar{K}^*$ | 0.01 | 0.07 | 0.26 | 0.74 | 1.83 |
| $K^*\bar{K}^*$ | 0.01 | 0.02 | 0.11 | 0.33 | 0.87 |
| Total | 0.10 | 0.50 | 1.77 | 5.06 | 12.43 |

Sizable!

$$\mathcal{BR}(K\bar{K})/\mathcal{BR}(\rho\pi) = (2.5 - 3.0) \times 10^{-1},$$
$$\mathcal{BR}(\omega\eta)/\mathcal{BR}(\rho\pi) = 8.9 \times 10^{-2},$$
$$\mathcal{BR}(\omega\eta')/\mathcal{BR}(\rho\pi) = (8.4 - 8.6) \times 10^{-3},$$
$$\mathcal{BR}(K\bar{K}^*)/\mathcal{BR}(\rho\pi) = 2.5 \times 10^{-1},$$
$$\mathcal{BR}(K^*\bar{K}^*)/\mathcal{BR}(\rho\pi) = (9.5 - 12.0) \times 10^{-2}.$$

Bai, Lai, Zhou, XL, arXiv:2412.09408

# 5. Non-$D\bar{D}$ decays of $\psi_3(3842)$

Evidence of $\psi_3(3842)$ from BESIII

PHYSICAL REVIEW D **106**, 052012 (2022)

With the update of BESIII, it is possible to find the non-$D\bar{D}$ decays of $\psi_3(3842)$

## Measurement of $e^+e^- \to \pi^+\pi^-D^+D^-$ cross sections at center-of-mass energies from 4.190 to 4.946 GeV

Using data samples collected with the BESIII detector operating at the BEPCII storage ring, we measure the cross sections of the $e^+e^- \to \pi^+\pi^-D^+D^-$ process at center-of-mass energies from 4.190 to 4.946 GeV with a partial reconstruction method. Resonance structures are seen and the cross section line shape can be described by the coherent sum of either two Breit-Wigner functions or a Breit-Wigner function and a phase space term. The mass and width of the resonance at about 4.4 GeV are determined to be $(4371.6 \pm 2.5 \pm 9.2)$ MeV$/c^2$ and $(167 \pm 4 \pm 29)$ MeV, respectively, which are in agreement with those of the $\psi(4360)$ or $Y(4390)$ state. The spin-3$D$-wave charmonium state $X(3842)$ is searched for through the $e^+e^- \to \pi^+\pi^-X(3842) \to \pi^+\pi^-D^+D^-$ process, and evidence with a significance of $4.2\sigma$ is found in the data samples with center-of-mass energies from 4.6 to 4.7 GeV.

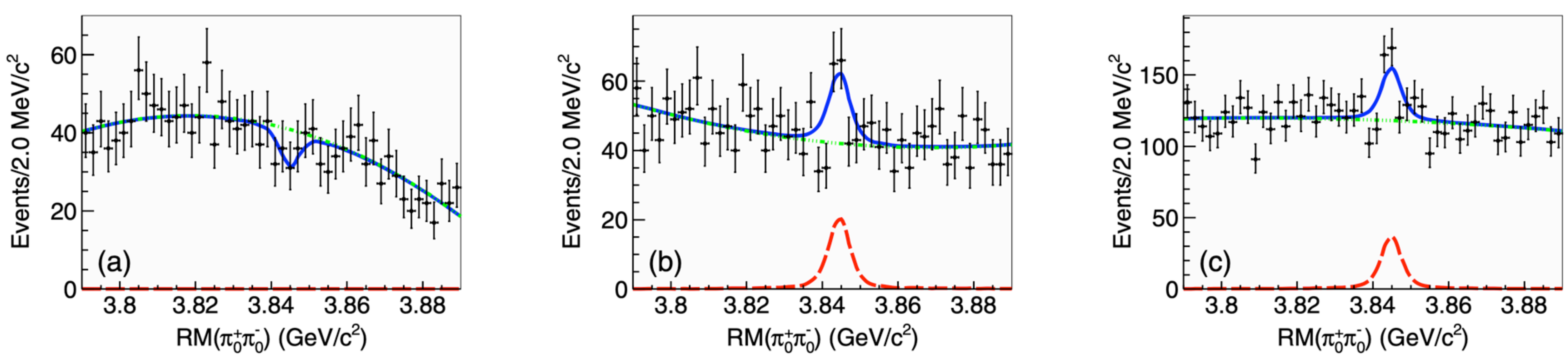


FIG. 9. The $RM(\pi_d^+\pi_d^-)$ distributions and the fits at $\sqrt{s} = 4.420$ (a), 4.680 (b) GeV, and data samples with $\sqrt{s}$ from 4.600 to 4.700 GeV (c). The black dots with error bars are the $S$ sample, and the red dashed, green dash-dotted, and blue solid curves are the

# 6. Summary

- XYZ states—Searching for exotic states is still a key issue
- We still need to pay more attention to the study of charmonium, especially for their high-lying states
- Unquenched effect & high precision hadron spectroscopy
- Theoretical + Experimental

Figure 1. Exotic hidden-heavy hadrons and other fantastic beasts (image by Jam-Di, deviantart.com/jam-di).

E. Braaten, R. Bruschini, arXiv:2409.08002

Quenched


Unquenched

# Thank you for your attention!